810 *Biochemistry* **2010,** *49,* 810–820
DOI: 10.1021/bi9015956

BIOCHEMISTRY
including biophysical chemistry & molecular biology
Article

Thiol−Disulfide Exchange between Glutaredoxin and Glutathione[†]

Rasmus Iversen, Peter Anders Andersen, Kristine Steen Jensen, Jakob R. Winther, and Bent W. Sigurskjold*

Department of Biology, University of Copenhagen, Copenhagen Biocenter, Ole Maaløes Vej 5, DK-2200 Copenhagen N, Denmark

Received September 11, 2009; Revised Manuscript Received November 18, 2009

ABSTRACT: Glutaredoxins are ubiquitous thiol−disulfide oxidoreductases which catalyze the reduction of glutathione−protein mixed disulfides. Belonging to the thioredoxin family, they contain a conserved active site CXXC motif. The N-proximal active site cysteine can form a mixed disulfide with glutathione or an intramolecular disulfide with the C-proximal cysteine. The C-proximal cysteine is not known to be involved in the catalytic mechanism. The stability of the mixed disulfide with glutathione has been investigated in detail using a mutant variant of yeast glutaredoxin 1, in which the C-proximal active site cysteine has been replaced with serine. The exchange reaction between the reduced protein and oxidized glutathione leading to formation of the mixed disulfide could readily be monitored by isothermal titration calorimetry (ITC) due to the enthalpic contributions from the noncovalent interactions and the protonation of glutathione thiolate. An algorithm for the analysis of this type of reaction by ITC was developed and showed that the interaction is enthalpy driven with a large entropy penalty. The applicability of the method was verified by a mass spectrometry-based approach, which gave a standard reduction potential of −295 mV for the mixed disulfide. In another set of experiments, the pK_a value of the active site cysteine was determined. In line with what has been observed for other glutaredoxins, this cysteine was found to have a very low pK_a value. The glutathionylation of glutaredoxin was shown to have a substantial effect on the thermal stability of the protein as revealed by differential scanning calorimetry.

In most cells glutathione (γ-GluCysGly) is present in millimolar amounts, making it the most abundant intramolecular small-molecule thiol (*1*). It is present throughout cellular compartments where it acts as an important antioxidizing agent in maintaining constant redox environments. In the cytosol, glutathione is kept in the reduced state (GSH)[1] through constant action of the enzyme glutathione reductase, which catalyzes the reduction of glutathione disulfide (GSSG) by NADPH. GSH functions as a reducing agent and a radical scavenger. One of its primary roles is to prevent irreversible damage caused by reactive oxygen species (*2*−*4*). During oxidative stress oxidized forms of cysteine thiols, such as sulfenic acids (−SOH), can be formed. Sulfenic acids are unstable and are easily oxidized further to sulfinic ($-SO_2H$) or sulfonic ($-SO_3H$) acids. These modifications are often considered irreversible and can therefore cause permanent damage to proteins (*5*). However, sulfenic acids also readily react with thiols to form disulfides. Since GSH is such an abundant thiol, oxidative stress therefore leads to the formation of mixed disulfides between protein cysteines and glutathione (*5*−*7*). This process of so-called S-glutathionylation can be seen as a way of protecting protein thiols from being oxidized irreversibly. Another suggested function of glutathionylation is as a mode of regulation since glutathionylation has been seen to efficiently alter the activity of certain enzymes and transcription factors (*5*). Also, glutathionylation has been observed as a response to normal signaling events not related to stress conditions (*8*). Whether glutathionylation mediates protection or regulation, the modification needs to be removed when oxidative stress or a signaling event is over. This process of *de*glutathionylation may be catalyzed by glutaredoxin (Grx) under appropriate redox conditions (*9*).

Grxs are small (9−15 kDa) ubiquitous thiol−disulfide oxidoreductases, which reduce disulfides through thiol−disulfide exchange reactions (*10*). They are members of the thioredoxin superfamily of proteins, and as many other members of this family they contain an active site CXXC motif (Grxs usually have the active site sequence CPYC). In contrast to thioredoxins, which act as general reductases, Grxs have been found to react specifically with glutathione-containing disulfides (*9*, *11*). During the reaction with an S-glutathionylated protein, the N-proximal active site cysteine of the Grx engages in a nucleophilic attack on the target disulfide leading to the breakage of the original mixed disulfide and concomitant transfer of the glutathione moiety to the Grx, so that the enzyme itself becomes glutathionylated and the reduced target protein is released. Afterward, the reduced active form of the Grx is reestablished by GSH-mediated reduction of the mixed disulfide (Figure 1) (*10*, *11*). The basis for the specificity of Grxs has been investigated by determination of the three-dimensional structures of several different Grxs in complex with glutathione (*12*−*17*). In all cases, a specific binding

[†]This work was supported by the Danish Natural Science Research Council. R.I. was supported by a Novo Nordisk Student Scholarship.

*Corresponding author. Phone: +45 3532 2068. Fax: +45 3532 2128. E-mail: bwsigurskjold@bio.ku.dk.

[1]Abbreviations: DoF, degrees of freedom; DSC, differential scanning calorimetry; DTNB, 5,5′-dithiobis(2-nitrobenzoic acid); DTT, dithiothreitol; Grx, glutaredoxin; Grx1p, Grx 1 from yeast; sCGrx1p, the single cysteine mutant of Grx1p (C30S); GrxSH, reduced sCGrx1p; GrxSSG, glutathionylated sCGrx1p; GSH, reduced glutathione; GSSG, oxidized glutathione; HPLC, high-performance liquid chromatography; IAM, iodoacetamide; ITC, isothermal titration calorimetry; mPEG-mal, methoxypolyethylene glycol 5000 maleimide; MALDI-TOF, matrix-assisted laser desorption/ionization time of flight; MS, mass spectrometry; SDS−PAGE, sodium dodecyl sulfate−polyacrylamide gel electrophoresis; TCA, trichloroacetic acid; TFA, trifluoroacetic acid; THP, tris(hydroxypropyl)phosphine.

 Published on Web 12/07/2009

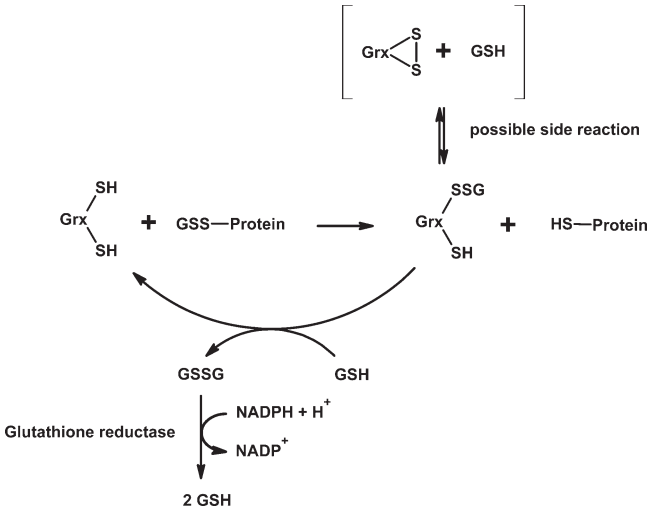

FIGURE 1: Schematic representation of the reaction mechanism used by glutaredoxins (Grxs). As shown, Grxs ultimately rely on reducing power of NADPH. In principle, the reactions can proceed in both directions, but for simplicity only the arrows that are physiologically relevant are shown. The enzyme reacts by a ping-pong mechanism in which a mixed disulfide is formed as an intermediate. The brackets indicate the possible off-pathway formation of an intramolecular disulfide.

pocket containing several conserved glutathione interaction partners has been revealed.

As shown in Figure 1, the C-proximal active site cysteine does not participate in the process of Grx-catalyzed deglutathionylation. This has been confirmed by the observation that mutant Grxs, which have the C-proximal cysteine replaced by serine, retain enzymatic activity (*16*−*19*) and in some cases have even higher activities than the wild-type enzymes (*16*, *17*, *19*). Although the C-proximal cysteine is not directly involved in deglutathionylation, it is able to attack the mixed disulfide with glutathione so that an intramolecular disulfide is formed between the two cysteines in the CXXC motif (Figure 1). Previous studies have suggested that this reaction is slow, though, and its significance is as yet unknown (*19*). Why is the second cysteine then conserved among Grxs? One explanation could be that it is necessary in order for Grxs to be able to reduce specific substrates other than glutathione-containing disulfides. Thus, Grxs were originally discovered in *Escherichia coli* as enzymes that catalyze the reduction of ribonucleotide reductase in a way that requires both cysteines in the active site (*18*, *20*). However, mouse Grx 2 has recently been shown only to require the N-proximal cysteine for full activity, suggesting that this Grx and possibly other eukaryotic Grxs catalyze the reduction of ribonucleotide reductase via a glutathionylated intermediate (*11*). It has also been suggested that the buried C-proximal cysteine is there to protect the reactive solvent-exposed N-proximal cysteine from irreversible oxidation during oxidative stress (*21*). Thus, one can imagine that an intramolecular disulfide will quickly be formed from the sulfenic acid derivative of the N-proximal cysteine. Finally, the C-proximal cysteine has been implicated in modulating the reactivity of the N-proximal cysteine (*17*, *19*, *22*). In this respect, it is interesting that the mutation to CPYS has been shown to have opposite effects on the activities of yeast Grx 1 and Grx 2, where the Grx 1 C30S mutant is five times more active and the Grx 2 C30S mutant is five times less active than their respective wild types (*17*).

With the overall goal of increasing the understanding of the mechanisms underlying Grx-catalyzed deglutathionylation, we here present a characterization of Grx 1 from yeast (Grx1p). We wanted to investigate the stability of the mixed disulfide between the enzyme and glutathione, which should provide missing information about the redox properties of Grxs. In order to avoid the side reaction shown in Figure 1, a single-cysteine variant of Grx1p (sCGrx1p) in which the C-proximal active site cysteine, Cys30, has been changed to serine was used.

The thiol−disulfide exchange reaction between glutaredoxin and glutathione is

$$\mathrm{GrxSH} + \mathrm{GSSG} \overset{K_{ox}}{\rightleftharpoons} \mathrm{GrxSSG} + \mathrm{GSH} \qquad (1)$$

where K_{ox} is the equilibrium constant. In this reaction a disulfide bond is broken and another one formed, which would be expected to be associated with a very small enthalpy change. However, crystal structures of both the reduced (GrxSH) and glutathionylated (GrxSSG) form of this protein have been determined recently, and six electrostatic interactions between different groups in the glutathione molecule and conserved residues in sCGrx1p are formed (*13*, *17*). This implies that the reaction might be associated with a significant enthalpy change. In addition, the thiol group of Grx is deprotonated at the experimental pH 7.0 (*17*) and the thiol of glutathione is protonated (*23*), so eq 1 is more correctly stated as

$$\mathrm{GrxS^-} + \mathrm{GSSG} + \mathrm{H^+} \rightleftharpoons \mathrm{GrxSSG} + \mathrm{GSH} \qquad (2)$$

where the proton is donated by the buffer. Thus, the protonation of glutathione thiolate and deprotonation of the buffer will also contribute to the enthalpy change, and the overall reaction is expected to be measurable by calorimetry. The catalytically enhanced rate of the reaction makes it feasible to study the thiol−disulfide exchange by isothermal titration calorimetry (ITC). It is unconventional to use ITC for monitoring covalent chemistry, and since the reaction follows an exchange scheme, a new algorithm had to be developed for analysis of the data. These data were compared with data for the stability of the mixed disulfide obtained from mass spectrometry. Furthermore, we determined the pK_a value of the catalytic thiol since this is important for the magnitude of K_{ox} (*24*).

EXPERIMENTAL PROCEDURES

Materials. Methoxypolyethylene glycol 5000 maleimide (mPEG-mal) was from Nektar Therapeutics. Tris(hydroxypropyl)phosphine (THP) was purchased from Calbiochem, and sinapinic acid was from Fluka. Other chemicals were from Sigma Aldrich or Merck. NAP-5 and NAP-10 gel filtration columns were obtained from GE Healthcare.

Expression and Purification of sCGrx1p. The yeast glutaredoxin single cysteine mutant Grx1p C30S with the C-terminal His-tag extension LEHHHHHH (here simply referred to as sCGrx1p) was expressed and purified essentially as previously described (*19*). The protein was extracted from the strain BL21-(DE3) (Novagen) by two freeze/thaw cycles in 50 mM potassium phosphate, pH 7.0, and 0.3 M NaCl and subsequent sonication on ice. The resulting lysate was centrifuged (10000*g*, 25 min, 4 °C), and the supernatant was collected.

The protein was purified in the glutathionylated state by addition of GSH and GSSG to 1 and 5 mM, respectively. Afterward, the protein was purified on a column (1.8 × 10 cm) with TALON resin (Clontech) charged with Co^{2+} ions. After loading, the column was washed with 130 mL of 50 mM

potassium phosphate, pH 7.0, and 0.3 M NaCl at a flow rate of 1 mL min^{-1}. The protein was then eluted by applying a linear gradient from 0 to 150 mM imidazole in the same buffer over 100 mL. After the protein had been isolated, it was verified by sodium dodecyl sulfate−polyacrylamide gel electrophoresis (SDS−PAGE) that it was pure. Finally, the buffer was changed to 50 mM potassium phosphate, pH 7.0, by dialysis, and the protein was stored at −18 °C.

Preparation of Solutions for ITC. A 10 mM potassium phosphate buffer, pH 7.0, prepared from Milli-Q ultrapure water (18.2 MΩ cm^{-1}) was used. Oxygen was removed as thoroughly as possible by saturating with Ar for 45 min and then degassing the solution by stirring under vacuum for 15 min. This procedure was repeated, and finally the solution was saturated with Ar for 15 min.

A volume of 775 μL of the sCGrx1p stock (0.4 mM) was reduced by addition of 25 μL of 50 mM DTT followed by incubation for 15 min. DTT and GSH were afterward removed by gel filtration on a prepacked NAP-10 column. To avoid oxidation of the protein during filtration, the column was equilibrated with deoxygenated buffer, and filtration took place in a container, which had its atmosphere replaced by Ar. The protein was eluted in 2 mL, giving a protein concentration of approximately 0.15 mM; 1.5 mL was injected in the calorimeter, and the rest was used to determine the protein concentration. This was done by measuring absorbance at 280 nm and using a theoretical extinction coefficient of 5960 M^{-1} cm^{-1} (*25*).

Isothermal Titration Calorimetry (*ITC*). The ITC experiments were performed using an MCS isothermal titration calorimeter (MicroCal LLC, Northampton, MA) (*26*) with a cell volume of 1.32 mL. The titrations were carried out at 25 °C and a stirring rate of 400 rpm. The calorimeter was calibrated by electrical heat pulses. Before the ITC experiment could begin, the newly filtrated sample was degassed for another 12 min with stirring under vacuum, and the instrument had its sample cell filled with Ar. A 1.6 mM solution of GSSG was made in deoxygenated buffer. The initial injection of all experiments was 3 μL, which was discarded in the subsequent analysis, followed by 21 injections of 7 μL with 180 s between all injections. Baseline correction and peak integration were done by the Origin 7.0 software supplied by the instrument manufacturer.

Analysis of ITC Data. The exchange equilibrium in eq 1 can be represented by the more general scheme:

$$AB + CD \rightleftharpoons AC + BD \tag{3}$$

In the present case C and D are formally identical (the glutathionyl moiety), but no information of the actual chemical mechanism is embedded in an ITC model. The equilibrium constant for this reaction is

$$K = \frac{[AC][BD]}{[AB][CD]} \tag{4}$$

If it is assumed that the initial concentrations of the species on the right-hand side in eq 3 are both zero, then combining the mass preservation equations with the mass action eq 4 gives a quadratic equation, which may be solved (see Supporting Information for details)

$$[AC] = \frac{K}{2(K-1)}\left([A]_{tot} + [C]_{tot} \pm \sqrt{([A]_{tot} + [C]_{tot})^2 - \frac{4(K-1)[A]_{tot}[C]_{tot}}{K}}\right) \tag{5}$$

where $[A]_{tot}$ and $[C]_{tot}$ are the total (stoichiometric) concentrations of the species containing the moieties A and C in the sample cell, respectively. In eq 5 the plus sign in front of the square root pertains to $K < 1$ and the minus sign to $K > 1$. The heat change, q_i, after the ith injection is given by

$$q_i = V_{cell}\Delta H^\circ \Delta[AC]_i \tag{6}$$

where V_{cell} is the volume of the sample cell, ΔH° is the standard molar enthalpy change of the reaction, and $\Delta[AC]_i$ is the change in the concentration of AC ($= \Delta[BD]_i$). This is given by

$$\Delta[AC]_i = [AC]_i - [AC]_{i-1}\exp\left(-\frac{V_i}{V_{cell}}\right) \tag{7}$$

where V_i is the volume of the ith injection. The exponential expression in eq 7 is the dilution factor of the sample cell contents after the ith injection (*27*).

The apparent equilibrium constant and ΔH° for the exchange reaction were determined from the ITC isotherms by nonlinear least-squares regression analysis using eqs 5−7. The standard free energy change, ΔG°, and standard entropy change, ΔS°, were calculated from the standard thermodynamic relations:

$$\Delta G^\circ = -RT\ln K = \Delta H^\circ - T\Delta S^\circ \tag{8}$$

where R is the universal gas constant (8.3144 J mol^{-1} K^{-1}) and T is the absolute temperature.

An Origin Function Definition File called Exchange.fdf has been written to enable this analysis. This file and a PDF file with a more detailed description of the model are available as Supporting Information.

Mass Spectrometry (*MS*). K_{ox} was also determined by MS based on the 306 Da difference in mass between reduced and glutathionylated sCGrx1p and the peak areas that can be obtained from an MS experiment. The instrument used was a matrix-assisted laser desorption/ionization time-of-flight (MALDI-TOF) mass spectrometer of the type autoflex from Bruker Daltonics (Bremen, Germany). The applied matrix was prepared on the same day or the day before an experiment and was made by dissolving 1 mg of sinapinic acid in 50 μL of 0.2% (v/v) trifluoroacetic acid (TFA) and 50 μL of acetonitrile. Analysis of a sample was in each case done by mixing 1 μL of sample with 1 μL of matrix on a piece of Parafilm and applying 1 μL of the mix onto a target plate where it was allowed to dry before the target plate was loaded in the mass spectrometer. Results were always obtained by shooting on three different spots within the same sample. Even in completely oxidized samples, small amounts of reduced sCGrx1p were detected. This is probably caused by laser-induced breakage of approximately 5% of the disulfide bridges present in a sample. This artifact was corrected for when calculating the relative amounts of reduced and oxidized protein by assuming that a fraction (5%) of the disulfide bonds would always be broken by shooting.

To test if reduced and glutathionylated sCGrx1p fly equally well in an MS experiment, various mixtures of reduced and oxidized sCGrx1p were made and subjected to MS. The areas under the peaks corresponding to the reduced and glutathionylated protein were determined by numeric integration and used as a measure of the relative amounts of the two forms of sCGrx1p. Reduced sCGrx1p was prepared by mixing 15 μL of the oxidized protein stock (0.4 mM) with 2 μL of 50 mM DTT followed by incubation for 15 min. One sample volume of 1 M HCl was added to both the completely reduced and the completely oxidized

sample before they were mixed in different ratios. The final samples used for MS were diluted in 0.5 M HCl to a total protein concentration of 10 μM.

For determination of K_{ox}, sCGrx1p was incubated with different [GSH]/[GSSG] ratios, and the relative amounts of reduced and glutathionylated protein were in each case determined by MS as described above. The GSH solution used for all samples was freshly prepared by dissolving GSH to 50 mM in 50 mM potassium phosphate, pH 7.0, and 1 mM EDTA. The pH was readjusted to 7.0 by addition of 2 M NaOH, and the precise concentration of GSH was afterward determined with 5,5′-dithiobis(2-nitrobenzoic acid) (DTNB) by measuring absorbance at 412 nm and using an extinction coefficient of 14150 M^{-1} cm^{-1} (*28*). The amount of GSH (25 μL) was held constant in each sample, whereas the amount of GSSG was varied by addition of either a 0.5 M or a 50 mM stock solution. Since a freshly prepared solution of GSH contains a small amount of GSSG, high [GSH]/[GSSG] ratios were obtained by reducing some of the GSSG by addition of 5 mM THP to 50 μL of the GSH solution. Twenty-five microliters of 0.2 mM sCGrx1p was added to each mix of GSH and GSSG, whereas 50 μL was used for samples with added THP. sCGrx1p was allowed to equilibrate with the glutathione for 10 min before the reaction was quenched by addition of one sample volume of 1 M HCl. Samples for MS were made by taking 5 μL from each acid-quenched reaction and diluting it in 20 μL of 0.5 M HCl.

Determination of the [*GSH*]/[*GSSG*] *Ratio*. Since GSH was in big excess in all samples, the amount was assumed constant before and after equilibration with sCGrx1p and was thus determined from the initial reaction with DTNB. The amount of GSSG, on the other hand, was in many samples even smaller than the amount of protein. In order to obtain the precise amount of GSSG at equilibrium, a sample from each acid-quenched reaction mixture was analyzed by high-performance liquid chromatography (HPLC) using an AKTA purifier system (GE Healthcare) equipped with a Vydac (218TP5415) 4.6 × 150 mm C-18 reversed-phase column. Each sample was diluted in 0.5 M HCl to a final volume of 200 μL and then injected manually in the HPLC system. GSSG was eluted isocratically in 0.1% TFA after ~8 min at a flow rate of 1 mL/min. The elution was monitored by continuously measuring absorbance at 248 nm, and the amount of GSSG in each sample was quantified by determination of the area of a resulting peak on the chromatogram. The determined areas were converted to molar amounts by correlation with a standard curve of areas obtained from samples with known amounts of GSSG.

Differential Scanning Calorimetry (*DSC*). Protein unfolding thermodynamics was determined by DSC using a VP-DSC from MicroCal LLC (Northampton, MA) (*29*, *30*) with a cell volume of 0.52061 mL. A scan rate of 1 °C min^{-1} and an excess pressure of 2 bar were applied. The DSC cell was filled with Ar before solutions were injected. Before commencing the DSC experiments of the protein, blank scans were collected with buffer in both the reference and sample cells until two consecutive scans coincided. The last blank scan was subtracted from the sample scans. The reversibility of the thermal transitions was assessed by checking the reproducibility of the scan upon immediate cooling and rescanning. Thermograms were plotted, and unfolding temperatures (T_d, the temperature where 50% of the protein is unfolded), and enthalpy changes were determined using Origin 7.0 software supplied by the manufacturer.

For the thermal denaturation experiments both states of the glutaredoxin mutant were analyzed. The solutions were made the same way as for the ITC experiments with the only difference being that the final protein concentration was only 40 μM. For the glutathionylated state, a theoretical extinction coefficient of 6085 M^{-1} cm^{-1} was used in order to determine the concentration (*25*).

The unfolding temperatures and enthalpy changes obtained from the DSC experiments were used to calculate the equilibrium constants of unfolding (K_u) at 25 °C according to the van't Hoff equation

$$\frac{d \ln K_u}{d(1/T)} = -\frac{\Delta H^\circ}{R} \quad (9)$$

and the relationship between temperature and enthalpy change

$$\Delta H^\circ(T) = \Delta H^\circ(T_d) + \Delta C_p(T - T_d) \quad (10)$$

where the change in heat capacity, ΔC_p, is assumed to be independent of temperature. Substitution of eq 10 into eq 9 and integration from T_d to T yields

$$K_u(T) = \exp\left\{ -\frac{1}{R}\left[(\Delta H^\circ(T_d) - T_d \Delta C_p)\left(\frac{1}{T} - \frac{1}{T_d}\right) - \Delta C_p \ln\left(\frac{T}{T_d}\right)\right]\right\} \quad (11)$$

since $K_u(T_d) = 1$. Thus, from the DSC data and a calculated value of ΔC_p based on the changes in solvent-accessible polar and nonpolar surface area upon unfolding (see below), it is possible to calculate the equilibrium constants for the following reactions at any temperature:

$$\text{GrxSH} \rightleftharpoons \text{unfolded GrxSH} \quad (12)$$

and

$$\text{GrxSSG} \rightleftharpoons \text{unfolded GrxSSG} \quad (13)$$

If reactions in eqs 12 and 13 are combined with a third reaction

$$\text{unfolded GrxSH} + \text{GSSG} \rightleftharpoons \text{unfolded GrxSSG} + \text{GSH} \quad (14)$$

then a thermodynamic cycle is completed, and the reaction in eq 1 is obtained. The equilibrium constant for the thiol−disulfide exchange reaction shown in eq 14 may be assumed to have a value of 1, since unfolded Grx has lost all noncovalent interactions with bound glutathione and the mixed disulfide can therefore be assumed to have the same thermodynamic stability as the disulfide in GSSG. Hence, it is possible to estimate a value of K_{ox} from the DSC data alone. This K_{ox} is based solely on the noncovalent interactions between sCGrx1p and glutathione and does not account for the effect of thiol pK_a values on the stabilities of the disulfide bonds in GSSG and GrxSSG.

Calculation of Solvent-Accessible Surface Area. Calculations of the polar and nonpolar solvent-accessible surface areas of the folded and unfolded states of both forms of sCGrx1p were carried out using the ASACalc program (v.1.2) (*31*), which is based on the Lee and Richards algorithm (*32*). As input for the glutathionylated form, GrxSSG, was used its PDB file, 2jac.pdb (*13*), and as input for GrxSH was used an edited version of the PDB file for the sCGrx1p-rxYFP fusion protein, 2jad.pdb (*13*), in which the coordinates for rxYFP were deleted (the N-terminal 238 residues).

Determination of the Thiol pK_a Value. The pK_a value of the cysteine thiol in sCGrx1p was determined based on its reactivity with iodoacetamide (IAM) at different pH values. sCGrx1p (0.2 mM) was reduced by addition of an equal volume of 5 mM DTT followed by incubation for 15 min. Ten microliters of this solution was added to 85 μL of buffer followed by addition of 5 μL of 20 mM IAM. The reaction was allowed to take place for exactly 1 min before it was quenched by addition of 11 μL of 100% (w/v) trichloroacetic acid (TCA). Each sample was put on ice for 15 min and then centrifuged (16100*g*, 10 min, 4 °C). The pellet was dissolved by sonication in 50 μL of 2× SDS−PAGE sample buffer (0.1 M Tris-HCl, pH 6.8, 4% SDS, 0.2% (w/v) bromophenol blue, 20% (v/v) glycerol) containing 1 mM mPEG-mal, and the pH was adjusted by addition of 5 μL of 1 M Tris-HCl, pH 8.0. The samples were incubated for 30 min and then loaded on a high-Tris 15% polyacrylamide gel (*33*). After running, the gel was Coomassie stained, and the bands were quantified using the program ImageJ (http://rsb.info.nih.gov/ij/).

The buffers were all 0.1 M in concentration and were as follows: sodium citrate, pH 2 and 3; sodium acetate, pH 3.5, 4, and 4.5; MES, pH 5 and 6; potassium phosphate, pH 7; Tris-HCl, pH 8.

Investigation of the pH Dependence of K_{ox}. K_{ox} for sCGrx1p was determined by the MS method at different pH values. However, only a single [GSH]/[GSSG] ratio was used for each K_{ox} determination. The ratio used was obtained from dissolving GSH and not adding either GSSG or THP, which in this case gave a [GSH]/[GSSG] ratio of approximately 250:1. Thus, GSH was dissolved to 50 mM in 5 mM buffer, and the pH was adjusted to the appropriate values with 2 M NaOH. Twenty-five microliters of the GSH solution was mixed with 25 μL of 0.2 mM sCGrx1p, and the species were allowed to equilibrate for 20 min. Afterward, the reaction was quenched as before. MS analysis and determination of the exact [GSH]/[GSSG] ratio was done as described above. The buffers were the same as the ones described for the pK_a determination experiment, and the pH values were 3, 4, 5.1, 5.6, 6, and 8. The K_{ox} value at pH 7 was taken from the MS experiment described above.

RESULTS

Isothermal Titration Calorimetry (*ITC*). A representative thermogram and the corresponding isotherm for the titration of 0.126 mM GrxSH with 1.60 mM GSSG obtained at 25.1 °C are shown in Figure 2. The concentrations were chosen from initial trials to obtain suitably sigmoid exchange isotherms. The isotherms were fitted using a new algorithm based on the exchange scheme described herein, and the results are shown in Figure 2B. The titration of GrxSH with GSSG was done three times, and the thermodynamic parameters obtained from regression analysis using the Exchange algorithm are shown in Table 1. The reproducibility is reasonably good although the value of K_{ox} is not determined very accurately. The error estimates calculated as standard deviations of the averages are somewhat larger than the errors for each experiment. The results show that the reaction is enthalpy driven with a large unfavorable entropy penalty ($-T\Delta S^\circ = +17.9$ kJ mol^{-1}). This strongly unfavorable contribution from entropy to the glutathionylation reaction probably stems from conformational restrictions on the protein structure as well as lost translational, rotational, and conformational freedom of glutathione upon binding. The determined K_{ox} value of 105 indicates that a significant stabilization of the protein structure is imposed by the formation of the mixed disulfide.

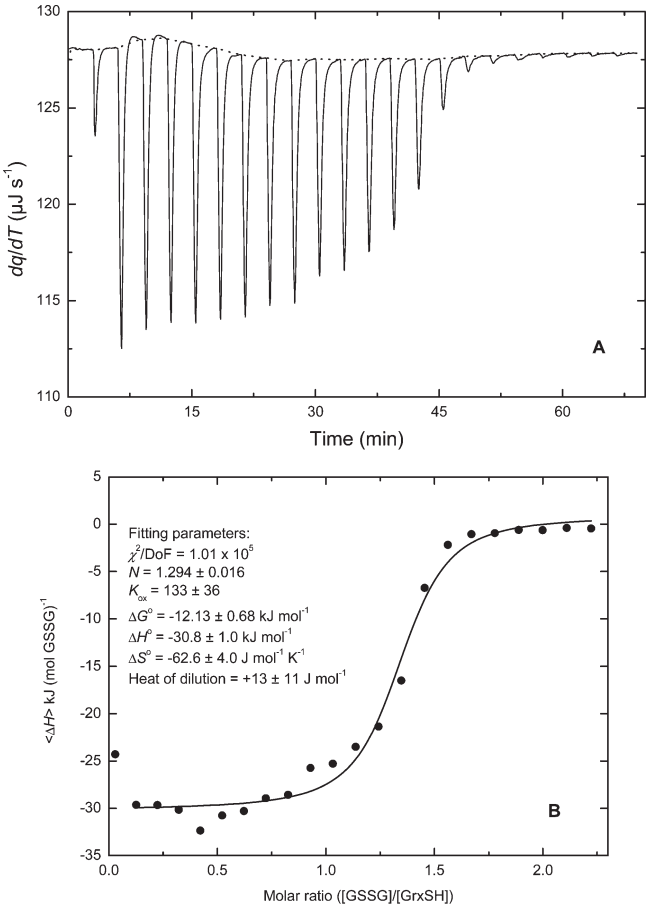

FIGURE 2: Isothermal titration calorimetric thermogram (A) and isotherm (B) for the glutathionylation of sCGrx1p. The dotted line in (A) is the adjusted calorimetric baseline. The solid line in (B) has been obtained from nonlinear least-squares regression to both the OneSites and the Exchange model (the regression lines from the two algorithms coincide). The first data point in (B) stems from the initial injection and was not used in fitting of the data.

The observed enthalpy change is the sum of contributions from breaking the disulfide bond in GSSG, forming the disulfide bond in GrxSSG, the formation of noncovalent interactions, the deprotonation of phosphate, and the protonation of glutathione thiolate (eq 2). The enthalpy change for protonation of glutathione thiolate is −32 kJ mol^{-1} (*23*), and ΔH° for deprotonation of dihydrogen phosphate is +3.6 kJ mol^{-1} (*34*). Breaking and making the disulfide bonds may be assumed to cancel out enthalpically, so by far most of the observed enthalpy change is due to the protonation of glutathione thiolate. The contribution to ΔH° from the noncovalent bonds is accordingly judged to be close to zero.

Determination of K_{ox} by MS. The value of K_{ox} was also determined by MS based on the 306 Da difference in mass between reduced and glutathionylated sCGrx1p. A representative example of a mass spectrum obtained from a mixture of reduced and glutathionylated sCGrx1p is shown in Figure 3A. It was verified that the two forms fly equally well in a MALDI-TOF experiment and thus that the peak areas obtained from the resulting spectrum can be used as a measure of the relative amounts of the two forms of the protein (Figure 3A, inset).

In order to determine K_{ox}, sCGrx1p was allowed to equilibrate with different ratios of [GSH]/[GSSG] at pH 7.0, and the distribution between reduced and glutathionylated protein was in each case determined by MS analysis after quenching of the

Table 1: Thermodynamic Data for Glutathionylation of Glutaredoxin Determined by Isothermal Titration Calorimetry and the Exchange Model

no.	temp (°C)	$[GrxSH]_0$ (mM)	$[GSSG]_{syringe}$ (mM)	N	K_{ox}	$\Delta G°$ (kJ mol^{-1})	$\Delta H°$ (kJ mol^{-1})	$\Delta S°$ (J mol^{-1} K^{-1})
1	25.1	0.126	1.60	1.29 ± 0.02	133 ± 36	−12.1 ± 0.7	−30.8 ± 1.0	−62.6 ± 4.0
2	25.1	0.156	1.81	1.13 ± 0.02	69 ± 25	−10.1 ± 0.9	−28.4 ± 1.3	−59.9 ± 5.2
3	25.1	0.156	1.81	1.31 ± 0.04	112 ± 59	−11.7 ± 1.3	−25.7 ± 1.9	−47.1 ± 7.8
average				1.24 ± 0.10	105 ± 33	−11.3 ± 1.1	−28.3 ± 2.6	−56.5 ± 8.3

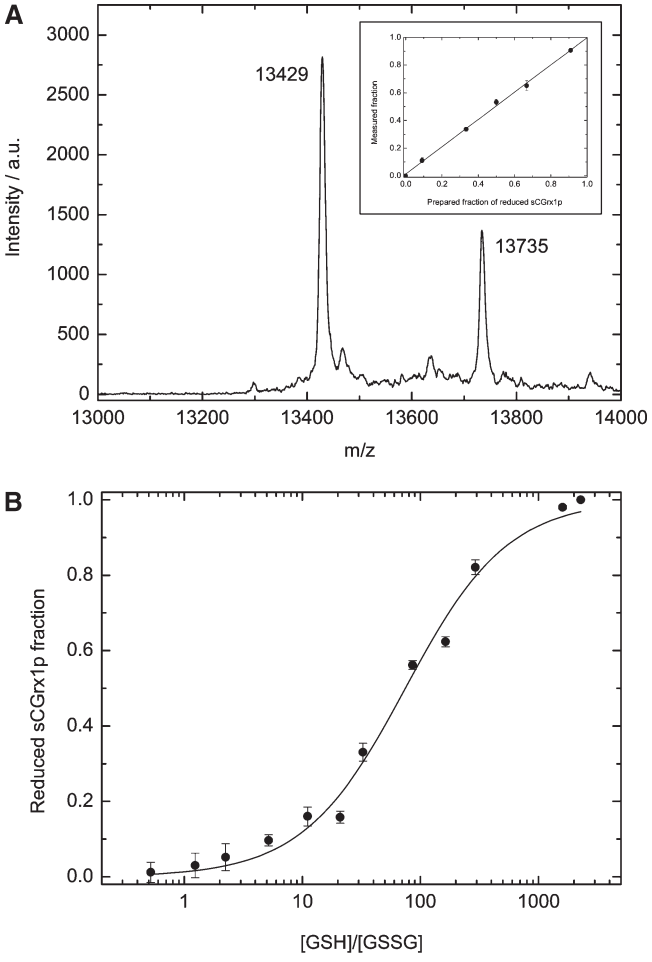

FIGURE 3: Mass spectrometric analysis of the distribution between reduced and glutathionylated sCGrx1p. An example of a spectrum obtained from a mixture of the two forms is shown in (A). The spectrum is zoomed in on the two resulting peaks at mass/charge ratios of 13429 and 13735 corresponding to reduced and glutathionylated sCGrx1p, respectively. The inset shows that the two forms fly equally well in a MALDI-TOF experiment. The fraction of reduced protein measured by MS was plotted against the fraction that was actually prepared. Linear regression gave a slope of 1. (B) The fraction of reduced sCGrx1p that was measured by MS after equilibration with a glutathione buffer was plotted against the [GSH]/[GSSG] ratio. K_{ox} was obtained from nonlinear least-squares regression (solid line). The fraction of reduced sCGrx1p is plotted as a mean ± SD obtained from three different measurements on the same sample.

reaction with HCl. The fraction of sCGrx1p in the reduced state was determined in each case and plotted against the [GSH]/[GSSG] ratio (Figure 3B). K_{ox} was determined after nonlinear least-squares regression according to the relation:

$$\frac{[GrxSH]}{[GrxSH]+[GrxSSG]} = \frac{\frac{[GSH]}{[GSSG]}}{\frac{[GSH]}{[GSSG]}+K_{ox}} \qquad (15)$$

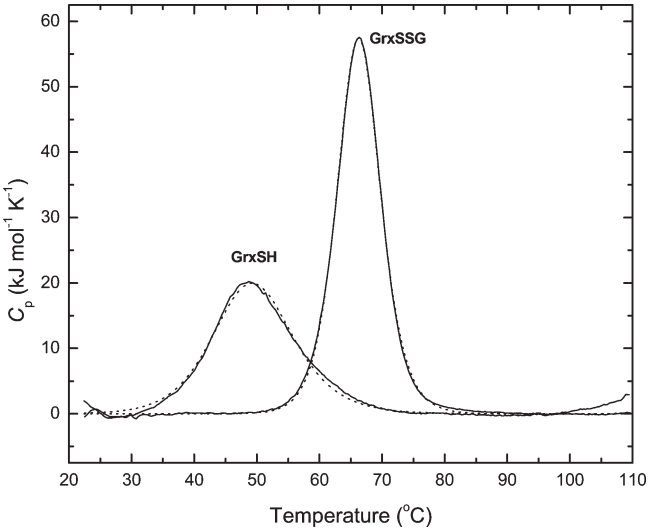

FIGURE 4: Differential scanning calorimetry of the unfolding of the reduced (left solid curve) and glutathionylated (right solid curve) form of sCGrx1p. The unfolding transitions have been fitted to a non-two-state unfolding mechanism (dotted curves).

which can be derived from the equilibrium expression for the reaction in eq 1. This gave a K_{ox} value of 74 ± 6, which is within the same range as the values determined by ITC.

Differential Scanning Calorimetry (*DSC*). In order to investigate further the stabilizing interactions between sCGrx1p and glutathione, the thermal stabilities of both GrxSH and the glutathionylated form, GrxSSG, were determined by DSC. Experiments for both GrxSH and GrxSSG were carried out in the absence of free glutathione. One peak was observed for each species at 49.5 °C for GrxSH (Figure 4, left curve) and at 66.3 °C for GrxSSG (Figure 4, right curve). No reversibility of unfolding was observed when the samples were rescanned after heating to 100 °C. However, repeated scans in the temperature range 20−62 °C for GrxSH and 20−72 °C for GrxSSG were recorded, and full reversibility of unfolding was observed for both forms (data not shown). It is thus appropriate to analyze the DSC data using reversible thermodynamics.

The DSC peaks were fitted to the standard non-two-state unfolding mechanism routines by Origin 7.0, and the obtained fits are shown as dotted lines in Figure 4. Table 2 shows the denaturation temperatures, the calorimetric enthalpy change of unfolding determined as the peak areas, $\Delta H°_{cal}$, and the van't Hoff enthalpy changes, $\Delta H°_{vH}$, determined from the peak shapes assuming a two-state transition. The fits show that the unfolding of both forms cannot quite be characterized as a two-state transition but seems to go through an intermediate state. The substantial difference in T_d of about 17 °C indicates that the association of the three amino acid residues from glutathione imposes a quite strong stabilizing effect on the protein structure. This stabilization must entirely or almost entirely result from the noncovalent interactions.

Table 2: Unfolding Thermodynamics of Reduced and Glutathionylated Glutaredoxin Determined by Differential Scanning Calorimetry and Structure-Based Calculations of Accessible Surface Areas

	GrxSH	GrxSSG
T_d (°C)	49.48 ± 0.05	66.32 ± 0.01
$\Delta H°_{cal}$ (kJ mol^{-1})	340 ± 2	531 ± 1
$\Delta H°_{vH}$ (kJ mol^{-1})[a]	203 ± 2	415 ± 1
$\Delta H°_{vH}/\Delta H°_{cal}$	0.60 ± 0.01	0.78 ± 0.01
$A^{folded}_{nonpolar}$ (Å^2)	3509	3293
$A^{unfolded}_{nonpolar}$ (Å^2)	9341	9469
$\Delta A_{nonpolar}$ (Å^2)[b]	5832	6176
A^{folded}_{polar} (Å^2)	2788	2638
$A^{unfolded}_{polar}$ (Å^2)	6477	6720
ΔA_{polar} (Å^2)[b]	3689	4082
ΔC_p(predicted) (kJ mol^{-1} K^{-1})	6.9	7.2
K_u (25 °C)	4.3×10^{-4}	9.7×10^{-9}

[a]The van't Hoff enthalpy change of unfolding assuming a two-state transition. [b]Calculation of changes in polar and nonpolar solvent-accessible surface areas of the unfolding of glutaredoxin on the basis of the crystal structures enables predictions of the thermodynamic values of the unfolding.

Calculations of solvent-accessible polar and nonpolar surface areas of the folded and unfolded states of both forms using the ASACalc v1.2 software give the values listed in Table 2. Glutathionylation results in a slight decrease in the polar surface area and a larger decrease in the nonpolar surface area of the folded form. On the basis of the changes of these areas upon unfolding, the heat capacity change between the folded and unfolded states, ΔC_p, can be estimated from the following empirical relation assuming complete unfolding (*35*):

$$\Delta C_p = c_n \Delta A_{nonpolar} + c_p \Delta A_{polar} \quad (16)$$

where the area changes are in Å^2 and $c_n = 1.88$ and $c_p = -1.09$ J mol^{-1} K^{-1} Å^{-2}, respectively.

As described in Experimental Procedures, K_{ox} can be estimated from the DSC experiments based on calculations of the equilibrium constants of unfolding at 25 °C for GrxSH and GrxSSG ($K_{ox} = K_u^{GrxSH}/K_u^{GrxSSG}$). The determined equilibrium constants obtained from the measured values for T_d and $\Delta H°$ and the calculated values for ΔC_p are given in Table 2. By this approach a K_{ox} value of 4.4×10^4 was obtained when the calorimetric enthalpy changes (ΔH_{cal}) are used and 5.3×10^4 when the van't Hoff enthalpy changes are used. It has thus little effect which enthalpy is used in the calculations. The calculation of K_u depends on ΔC_p. If eq 11 is differentiated with respect to ΔC_p, then $\partial K_u/\partial \Delta C_p$ is 1.7×10^{-7} and 1.0×10^{-11} mol K J^{-1} at 25 °C for GrxSH and GrxSSG, respectively. These values are both small compared to K_u. ΔC_p could also have been estimated from the shifts in the baselines of the DSC scans, but that method is very uncertain. Another way to estimate ΔC_p is by dividing the difference in $\Delta H°_{cal}$ for the unfolding of GrxSH and GrxSSG with the difference in T_d, which gives 11.3 kJ mol^{-1} K^{-1}. This is somewhat larger than ΔC_p calculated from the surface areas and may suggest that these are underestimated. However, using $\Delta C_p = 11.3$ kJ mol^{-1} K^{-1} in eq 11 yields values of K_u of 2.3×10^{-3} and 7.5×10^{-7} for GrxSH and GrxSSG, respectively, and an apparent $K_{ox} = 3.1 \times 10^3$. These differences are within a reasonable range of uncertainty. K_{ox} derived from DSC is much larger than what was determined by both ITC and MS, but here it should be noted that the value obtained from the DSC data only reflects the noncovalent interactions that stabilize the mixed disulfide between sCGrx1p and glutathione and does not take the effect of thiol pK_a values on the stability of disulfide bonds into consideration. A lower pK_a of GrxSH compared to GSH will destabilize the mixed disulfide in GrxSSG compared to the GSSG disulfide because a more stable thiolate anion has decreased nucleophilic character and at the same time better leaving group abilities (*24*). Thus, the K_{ox} value determined from the DSC experiments can be seen as the K_{ox} that would be expected if GrxSH and GSH had equal thiol pK_a values.

The Thiol pK_a Value of sCGrx1p. The data obtained from the DSC experiments together with the K_{ox} values that were determined from ITC and MS indicate that the cysteine residue in GrxSH has a pK_a value, which is substantially lower than the pK_a value of the cysteine in GSH. This would be consistent with what has been found for other Grxs for which pK_a values as low as 3.5 have been reported for the N-proximal cysteine in the active site (*17*, *22*, *36*−*38*). In order to estimate the pK_a value of the one cysteine residue in sCGrx1p, we investigated the reactivity of GrxSH with the small alkylating agent IAM at different pH values. After incubation for exactly 1 min, the reaction was quenched by acidification and precipitation of the protein with TCA. GrxSH that had not reacted with IAM was in each case modified with another alkylating agent, mPEG-mal, which adds 5 kDa to the molecular mass of the protein. Thus, the two differently modified forms of sCGrx1p can be separated on a polyacrylamide gel (Figure 5A). In fact, the observable shift in mobility that mPEG-mal produces is even larger than what would be expected from its mass because of extensive water binding by the polyethylene glycol chain. The amount of protein that had reacted with IAM and therefore unreactive toward mPEG-mal was determined by quantification of the intensities of the Coomassie-stained protein bands.

Since IAM was in large excess over GrxSH, the reaction can be analyzed as a pseudo-first-order reaction. The observable second-order rate constant, k_{obs}, for the alkylation of GrxSH by IAM was calculated at each pH value from the fraction of the protein that was reactive toward mPEG-mal. Since it is the thiolate anion that acts as a nucleophile in the reaction, the reactivity at a given pH depends on the pK_a value of the cysteine. The relationship between pH and k_{obs} is given by the expression

$$k_{obs} = \frac{k_{S^-}}{1 + 10^{pK_a - pH}} \quad (17)$$

where k_{S^-} is the rate constant for the reaction between the thiolate anion and IAM. According to this relationship, plotting k_{obs} against pH should give a single transition at a pH equal to the cysteine pK_a value (Figure 5B). The values for the fit are pK_a = 4.5 ± 0.1 and $k_{S^-} = 44 \pm 2$ M^{-1} s^{-1} (reduced $\chi^2 = 7.3$), which clearly shows that the cysteine in sCGrx1p does in fact have a much lower pK_a value than the cysteine in GSH, which according to previous studies has a pK_a of 8.9 (*39*). The pK_a value determined here is somewhat higher than what was recently found for yeast wild-type Grx 1 by Discola et al. (*17*). They used two different approaches to determine the pK_a value of the N-proximal cysteine: enzyme inhibition with IAM and alkylation with monobromobimane at different pH values giving pK_a values of 4.0 and 3.2, respectively. One possible explanation for our pK_a value being higher might be found in the data presented in Figure 5. Although the significance is questionable, the appearance of the data points in Figure 5B could imply two transitions instead of one, suggesting that something else might be titrating in a way that affects the nucleophilicity of Cys27. Also, the large

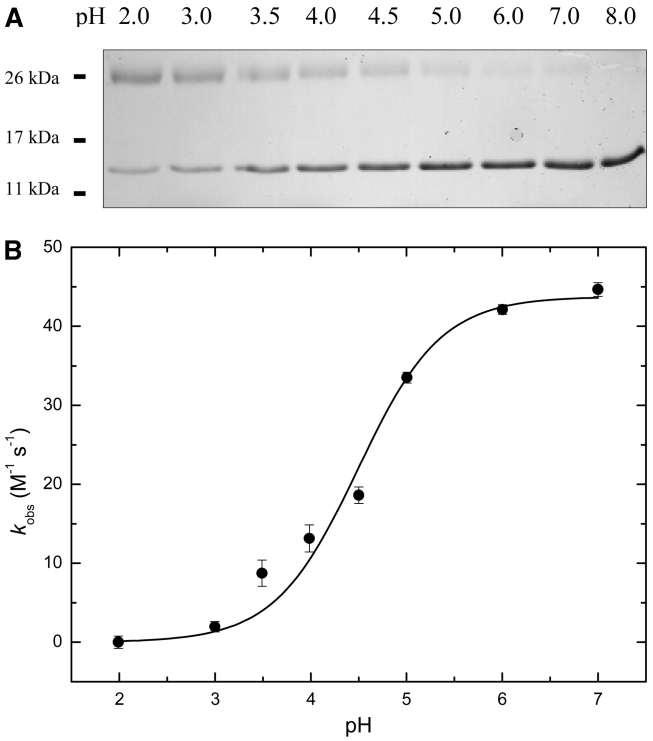

FIGURE 5: Determination of the pK_a value of Cys27. (A) Coomassie-stained SDS−PAGE gel where the number above each lane is the pH value at which sCGrx1p and IAM were incubated. sCGrx1p that had not reacted with IAM (~26 kDa band) was separated from sCGrx1p that had reacted with IAM (~14 kDa band) by modification with mPEG-mal followed by SDS−PAGE. At the lowest pH values, sCGrx1p is expected to be unreactive toward IAM and thus fully modified by mPEG-mal. This is not exactly what is seen, since a fraction of the protein has not reacted with mPEG-mal. We suspect that this incomplete modification was due to either partial oxygen oxidation during the preparation or the presence of free maleimide in the mPEG-mal. We assumed that the same fraction of protein was unmodified in all samples and corrected for this in the calculation of k_{obs}. (B) k_{obs} was calculated from the intensity of the gel bands for pH values 2−7 and plotted against pH. The pK_a value of Cys27 and k_{S^-} were then obtained by nonlinear least-squares regression using a single transition model. k_{obs} is plotted as a mean obtained from two independent experiments.

rate constant that is reached at neutral pH supports the idea that a different group increases the nucleophilicity of the thiolate (*40*). If the data are instead fitted to a two-state model, pK_a values of 3.3 ± 0.7 and 4.8 ± 0.2 are obtained (data not shown), where the low value would be the true pK_a of the cysteine. This fits well with the lower pK_a value that was found by Discola et al. (*17*). Importantly, their data are based on pH values lower than ~4.5, and a possible second transition cannot be seen. It should be stressed that the two-state model is somewhat speculative. However, with respect to the nucleophilicity of Cys27, our data imply an effective pK_a of around 4.5, regardless of the model.

Relationship between pH and K_{ox}. Since GrxSH and GSH have different thiol pK_a values, the reaction between GrxSH and GSSG will take up one proton if it takes place at a pH value between the two pK_a values. This implies that K_{ox} should increase by a factor of 10 for each unit the pH is decreased between pH ~9 and pH ~5. In order to investigate this relationship, K_{ox} was estimated at different pH values by the MS method.

If the observable forward and reverse rate constants associated with the equilibrium given in eq 1 are named $k_{on,obs}$ and $k_{off,obs}$, respectively, then the logarithm of K_{ox} can be

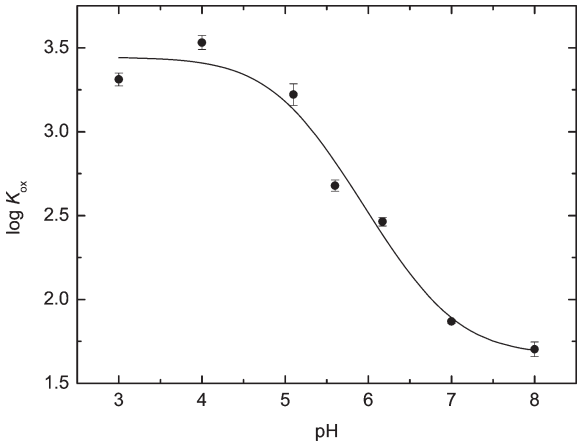

FIGURE 6: Dependence of K_{ox} on pH. The logarithm of K_{ox} was determined at different pH values by the MS method using a single [GSH]/[GSSG] ratio of approximately 250:1. The obtained values were plotted against pH as means ± SD obtained from three different measurements on each sample. The cysteine pK_a values of GrxSH and GSH along with the value of log($k_{on,S^-}/k_{off,S^-}$) were obtained by nonlinear least-squares regression (solid line).

expressed as

$$\log K_{ox} = \log k_{on,obs} - \log k_{off,obs} = \log \frac{k_{on,S^-}}{1+10^{pK_a(GrxSH)-pH}} - \log \frac{k_{off,S^-}}{1+10^{pK_a(GSH)-pH}} = \log \frac{1+10^{pK_a(GSH)-pH}}{1+10^{pK_a(GrxSH)-pH}} + \log \frac{k_{on,S^-}}{k_{off,S^-}} \quad (18)$$

Since it is the thiolate anion that acts as the nucleophile in both the forward and reverse reaction given in eq 1, the correlation given in eq 17 has been used to describe the reaction rates. Thus, k_{on,S^-} and k_{off,S^-} refer to the rate constants for the attack of the thiolate anions of GrxSH and GSH on GSSG and GrxSSG, respectively. Plotting the logarithm of K_{ox} against pH followed by nonlinear least-squares regression gave pK_a values of 5.1 ± 0.2 and 6.8 ± 0.2 for the cysteines in GrxSH and GSH, respectively (Figure 6). The value of log($k_{on,S^-}/k_{off,S^-}$) was determined to be 1.67 ± 0.12. The data points follow the expected trend nicely between pH ~5 and pH ~7. The pK_a value of 5.1 fits fairly well with what was determined for the sCGrx1p cysteine in Figure 5. The pK_a value of 6.8, on the other hand, is two pH units below the correct value for the GSH cysteine. This suggests that something else might be titrating in that area in a way that affects K_{ox}. This could be a histidine residue although no histidines are directly involved in glutathione binding. His31, however, sits close to Cys27 and could affect the nucleophilic character of the thiolate anion so that deprotonation will cause a destabilization that increases the nucleophilicity and decreases the leaving group ability of the thiolate. This is an unresolved issue, and it would have been desirable to apply the same experimental approach to other Grxs with known active site pK_a values in order to determine whether the problem with the apparent pK_a of GSH is peculiar to this form of Grx.

Although the reasons for the observed pH dependence remain to be determined in detail, it should be pointed out that many effects potentially could affect the pH dependence of K_{ox}. Furthermore, the strong pH dependence of K_{ox} between pH 5 and pH 7 confirms the much lower pK_a value of the GrxSH thiol compared to the GSH thiol.

DISCUSSION

The use of ITC in the analysis of a thiol−disulfide exchange reaction between a monocysteine glutaredoxin mutant and oxidized glutathione was carried out successfully. This work has demonstrated the use of a novel regression function based on the exchange scheme for the analysis of ITC data. Fitting instead by the standard OneSites binding function of Origin yields regression curves that completely coincide with curves from the Exchange model, and the values for χ^2, stoichiometry (N), $\Delta H°$, and heat of dilution are the same. The two models have the same number of regression parameters and therefore the same number of degrees of freedom (DoF). The apparent binding constant obtained with the OneSites model is $(1.1 \pm 0.3) \times 10^6$ M^{-1}. This value is not only of the wrong dimension but also 4 orders of magnitude greater than K_{ox} obtained by the Exchange model. The erroneous value of the equilibrium constant by the OneSites model propagates into apparent values of $\Delta G° = -35.5 \pm 0.7$ kJ mol^{-1} and $\Delta S° = +11.4 \pm 4.1$ J mol^{-1} K^{-1}. It is important to emphasize that it is not possible to distinguish between the two models solely on the basis of ITC data, so independent knowledge of the molecular reaction scheme is necessary. Nor is it possible to infer any information regarding the chemical mechanism of a reaction from an ITC experiment. The standard binding model in the OneSites algorithm assumes a number of identical and independent binding sites on the protein and pertains to the reaction scheme A + B ⇋ AB, which typically describes an addition or a ligand binding interaction. The Exchange algorithm corresponds to the scheme AB + CD ⇋ AC + BD. The glutathionylation of GrxSH in eq 1 is an exchange reaction, and the Exchange model must therefore be the correct model to use here. Selection of a function that corresponds to the correct mass action expression is thus crucial when studying a specific reaction. Otherwise, a meaningless value for the equilibrium constant may be obtained, and as a consequence erroneous values of $\Delta G°$ and $\Delta S°$ are estimated. This may be relevant to take into account in many cases that may not be as obvious as the one described here. If, for instance, a binding interaction is accompanied by a protonation change, e.g., A + B ⇋ AB + H^+, then this is formally an exchange reaction and more appropriately analyzed by the Exchange model than by the standard binding model (OneSites). However, the protonation linkage will not significantly influence the determination of the equilibrium constant using the standard binding model (*41*). This also applies to eq 2 where there are three reactants on the left-hand side, but where [H^+] is constant and does not influence the equilibrium significantly. If, instead, a metal ion is released (A + B ⇋ AB + M^+), then a suitable chelator or other metal buffer must be present for the standard OneSites binding model to be employed. We have shown that sigmoid curves are obtained by the Exchange model for equilibrium constants in the range $5 < K < 10^4$ (Supporting Information). The equilibrium constant observed here ($K = 105$) is nicely within this range.

Noninteger values of the stoichiometry parameter N are due to uncertainties in the concentrations of protein and glutathione. The protein concentration has been determined spectrophotometrically using an absorption coefficient that was calculated from the amino acid composition (*25*), and this may underestimate the concentration. [GSSG] was also determined spectrophotometrically, but it is unlikely that this would be significantly overestimated. The molar enthalpy change is determined relative to the ligand concentration and is not affected by uncertainties in the protein concentration.

The K_{ox} value of 105 that was determined by ITC indicates a significant stabilization of the mixed disulfide between sCGrx1p and glutathione caused by favorable interactions between the protein and the bound glutathione moiety. In addition, the linked equilibrium of glutathione thiolate protonation further drives the reaction in eq 2 toward the right-hand side.

In contrast to K_{ox} determined by ITC, the apparent $K_{ox} = 4.4 \times 10^4$ determined by DSC stems from contributions from the noncovalent interactions only. This corresponds to $\Delta G°_{noncovalent} = -26.5$ kJ mol^{-1}, and since $\Delta H°_{noncovalent} \approx 0$ kJ mol^{-1}, then $\Delta S°_{noncovalent} = 89$ J mol^{-1} K^{-1}. This large favorable entropic contribution is probably due to the release of surface-bound water molecules into bulk solvent. The total entropy change is the sum of changes in covalent and noncovalent interactions plus changes in translational, rotational, and conformational entropy of Grx and GSH. It may be assumed that $\Delta S°_{covalent} \approx 0$, which means that the entropic penalty imposed by translational, rotational, and conformational restrictions is very large, ≈−146 J mol^{-1} K^{-1}. Elgán and Berndt recently reported a very detailed study where they dissect the noncovalent interactions between *E. coli* Grx 3 and glutathione (*42*). They used 14 synthetically modified analogues and derivatives of glutathione and determined their influence of their destabilizing or stabilizing effects on Grx 3 toward urea denaturation detected by circular dichroism spectroscopy. The reported free energy changes of folding can be used to calculate K_u values. If this is done for the free enzyme, a value of 3.6×10^{-4} is obtained. This corresponds closely to what we report in Table 2 for sCGrx1p (4.3×10^{-4}). Interestingly, however, the value of K_u for the glutathione-bound form of Grx 3 is only reduced to 1.5×10^{-4}, suggesting a much less stabilizing effect of the glutathionylation than what is reported here ($K_u = 9.7 \times 10^{-9}$). The denaturation approach using glutathione analogues does not give any information on the enthalpy or entropy of the interactions, and it would be very informative to apply ITC measurements on such analogues.

The applicability of the ITC method was in the present case demonstrated by confirming the determined value of the equilibrium constant, K_{ox}, by an MS-based approach. A value of 105 was determined by ITC, whereas MS analysis gave $K_{ox} = 74$. The MS experiments represent a more classic approach to determination of K_{ox} where the protein is incubated in different ratios of [GSH]/[GSSG] followed by determination of the degree of oxidation in each case. The ITC approach, on the other hand, obviates the need for construction of individual redox buffers. Although the K_{ox} value that was derived from MS is more accurately determined, the ITC method has the advantage that it produces additional thermodynamic information, which cannot easily be obtained otherwise.

The standard reduction potential for the mixed disulfide between sCGrx1p and glutathione can be calculated from the knowledge of the value of K_{ox} according to the Nernst equation

$$E°'_{GrxSSG} = E°'_{GSSG} - \frac{RT}{zF} \ln K \qquad (19)$$

where F is the Faraday constant (9.6485×10^4 J V^{-1} mol^{-1}) and $E°'_{GSSG}$ is the standard reduction potential for the GSSG disulfide. If a K_{ox} of 74 is used and $E°'_{GSSG}$ is set to −240 mV (*43*), then a standard reduction potential of −295 mV is obtained at 25 °C. To our knowledge this is the first reported value of the redox potential for the mixed disulfide between a Grx and glutathione. However, standard reduction potentials have been determined for the intramolecular disulfide in both

E. coli (*44*) and human (*45*) Grxs. For these disulfides, values ranging from −198 to −232 mV have been reported. When the standard reduction potentials of both the intramolecular disulfide and the mixed disulfide with glutathione are known, it is possible to calculate the equilibrium constant for the side reaction shown in Figure 1

$$\ln K = \frac{2F(E^{\circ\prime}_{\mathrm{Grx}_{\mathrm{SH}}^{\mathrm{SSG}}} - E^{\circ\prime}_{\mathrm{Grx}})}{RT} \quad (20)$$

As a model, the $E^{\circ\prime}$ value determined here for the mixed disulfide between sCGrx1p and glutathione can be used together with the −232 mV that has been reported for the intramolecular disulfide in human Grx 1 (*45*). This approach gives an equilibrium constant of 7.4×10^{-3} M. Assuming an intracellular GSH concentration of 10 mM, this means that the ratio between the amounts of intramolecular disulfide and mixed disulfide will be 0.74:1 at equilibrium; i.e., they will be present in almost equal amounts. However, according to experiments with the sensor rxYFP, the [GSH]/[GSSG] ratio in the yeast cytosol is of the order ~3000:1 (*46*), which means that the sum of the two oxidized forms will account for only ~4% of the total amount of enzyme at equilibrium. This makes sense, of course, since only reduced Grx is active in deglutathionylation.

In line with previous studies of other Grxs, the cysteine residue in sCGrx1p was found to have a very low pK_a value. The data presented in Figure 5 suggests that the pK_a value of Cys27 is around 4.5. The low pK_a value of the N-proximal cysteine in the active site of *E. coli* Grx 3 was suggested to result from stabilization of the thiolate anion by hydrogen bonds with two backbone amide hydrogen atoms as well as the thiol hydrogen of the C-proximal cysteine in the active site (*22*, *24*). Corresponding interactions can be found when studying the crystal structure of reduced sCGrx1p (PDB code 2JAD) where the thiolate anion is stabilized through hydrogen bonding with the backbone amide hydrogen atoms of Tyr29 and Ser30 as well as hydrogen bonding with the side chain hydroxyl group of Ser30.

Lowering the pK_a value of a thiol decreases the nucleophilic character and increases the leaving group ability of the corresponding thiolate anion. Both effects will make the sulfur atom less willing to be involved in disulfide bonding (*47*). On the other hand, if a thiol is to engage in a thiol−disulfide exchange reaction, it is a criterion that the thiolate anion is present since this is the reactive species (*24*). Thus, if a thiol should participate in disulfide bond formation, its pK_a value cannot be so high that no thiolate anions are present at the pH of the solution. All of these effects should be considered when trying to predict the dependence of K_{ox} on the pK_a of the cysteine in sCGrx1p.

The rate constant for the reaction between a thiolate anion and a disulfide can be described by a general Brønsted relation (*48*)

$$\log k_{S^-} = C + \beta_{\mathrm{nuc}} \mathrm{p}K_a^{\mathrm{nuc}} + \beta_C \mathrm{p}K_a^{\mathrm{C}} + \beta_{\mathrm{lg}} \mathrm{p}K_a^{\mathrm{lg}} \quad (21)$$

where C is a constant and pK_a^{nuc}, pK_a^{C}, and pK_a^{lg} are the pK_a values of the thiols that act as nucleophile, central thiol, and leaving group, respectively. Based on studies performed on small molecule thiols, Szajewski and Whitesides assigned values of 0.59, −0.4, and −0.59 to the Brønsted coefficients β_{nuc}, β_C, and β_{lg}, respectively (*48*). If these values are used and eqs 18 and 21 are combined, then it is possible to describe the theoretical relationship between the pK_a of Cys27 in sCGrx1p and K_{ox} (Figure 7). According to this relationship, changing the cysteine pK_a of sCGrx1p from 4.5 to 8.9 (the pK_a of the GSH cysteine) should result in an increase in K_{ox} from 74 to 1.4×10^5. This nicely explains the high value of K_{ox} that was estimated from the DSC data ($K_{ox} = 4.4 \times 10^4$) where only the noncovalent interactions which stabilize the glutathionylated form of sCGrx1p were considered. These interactions make sure that the Grx reacts specifically with glutathione-containing disulfides. At the same time they cause K_{ox} to become very high, though. Had K_{ox} been 4.4×10^4, the ratio between GrxSSG and GrxSH would be 15:1 at a [GSH]/[GSSG] ratio of 3000:1. Thus, in the cytosol most of the enzyme would be in the glutathionylated or oxidized state at equilibrium. The low pK_a of the N-proximal active site cysteine in Grxs can therefore be seen as a means for keeping K_{ox} relatively low and at the same time retain high specificity.

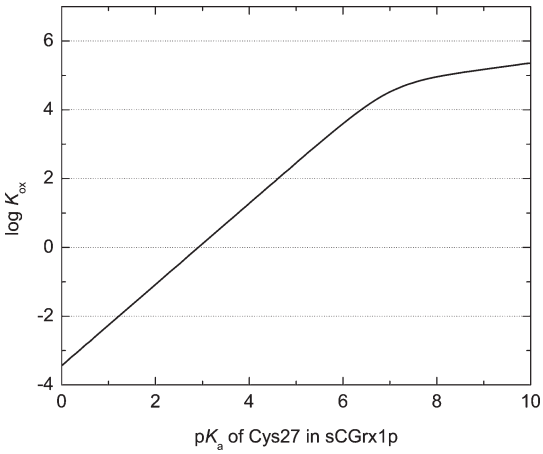

FIGURE 7: Expected relationship between the logarithm of K_{ox} and the cysteine pK_a of sCGrx1p at pH 7.0. The curve is based on eqs 18 and 21 and a fixed point at a pK_a value of 4.5 and a K_{ox} of 74.

ACKNOWLEDGMENT

We thank Svetlana Hansen for technical assistance and Professor Ernesto Freire for providing the ASACalc v.1.2 program.

SUPPORTING INFORMATION AVAILABLE

The Origin Function Definition File called Exchange.fdf for analysis of exchange reactions by ITC and a PDF file with instructions for installation and use of the Exchange algorithm. This material is available free of charge via the Internet at http://pubs.acs.org.

REFERENCES

1. López-Mirabel, H. R., and Winther, J. R. (2008) Redox Characteristics of the Eukaryotic Cytosol. *Biochim. Biophys. Acta 1783*, 629–640.
2. Anderson, M. E. (1998) Glutathione: An Overview of Biosynthesis and Modulation. *Chem.−Biol. Interact. 111−112*, 1–14.
3. Jones, C. M., Lawrence, A., Wardman, P., and Burkitt, M. J. (2003) Kinetics of Superoxide Scavenging by Glutathione: An Evaluation of Its Role in the Removal of Mitochondrial Superoxide. *Biochem. Soc. Trans. 31*, 1337–1339.
4. Stadtman, E. R. (1992) Protein Oxidation and Aging. *Science 257*, 1220–1224.
5. Ghezzi, P. (2005) Regulation of Protein Function by Glutathionylation. *Free Radical Res. 39*, 573–580.
6. Gallogly, M. M., and Mieyal, J. J. (2007) Mechanisms of Reversible Protein Glutathionylation in Redox Signaling and Oxidative Stress. *Curr. Opin. Pharmacol. 7*, 381–391.
7. Niwa, T. (2007) Protein Glutathionylation and Oxidative Stress. *J. Chromatogr. B 855*, 59–65.

8. Adachi, T., Pimentel, D. R., Heibeck, T., Hou, X., Lee, Y. J., Jiang, B., Ido, Y., and Cohen, R. A. (2004) *S*-Glutathionylation of Ras Mediates Redox-sensitive Signaling by Angiotensin II in Vascular Smooth Muscle Cells. *J. Biol. Chem. 279*, 29857–29862.
9. Gravina, S. A., and Mieyal, J. J. (1993) Thioltransferase Is a Specific Glutathionyl Mixed Disulfide Oxidoreductase. *Biochemistry 32*, 3368–3376.
10. Fernandes, A. P., and Holmgren, A. (2004) Glutaredoxins: Glutathione-Dependent Redox Enzymes with Functions far beyond a Simple Thioredoxin Backup System. *Antioxid. Redox Signaling 6*, 63–74.
11. Avval, F. Z., and Holmgren, A. (2009) Molecular Mechanisms of Thioredoxin and Glutaredoxin as Hydrogen Donors for Mammalian S Phase Ribonucleotide Reductase. *J. Biol. Chem. 284*, 8233–8240.
12. Bushweller, J. H., Billeter, M., Holmgren, A., and Wüthrich, K. (1994) The Nuclear Magnetic Resonance Solution Structure of the Mixed Disulfide between *Escherichia coli* Glutaredoxin(C14S) and Glutathione. *J. Mol. Biol. 235*, 1585–1597.
13. Hakansson, K. O., and Winther, J. R. (2007) Structure of Glutaredoxin Grx1p C30S Mutant from Yeast. *Acta Crystallogr. D63*, 288–294.
14. Nordstrand, K., Åslund, F., Holmgren, A., Otting, G., and Berndt, K. D. (1999) NMR Structure of *Escherichia coli* Glutaredoxin 3-Glutathione Mixed Disulfide Complex: Implications for the Enzymatic Mechanism. *J. Mol. Biol. 286*, 541–552.
15. Yu, J., Zhang, N.-N., Yin, P.-D., Cui, P.-X., and Zhou, C.-Z. (2008) Glutathionylation-Triggered Conformational Changes of Glutaredoxin Grx1 from the Yeast *Saccharomyces cerevisiae*. *Proteins 72*, 1077–1083.
16. Yang, Y., Jao, S., Nanduri, S., Starke, D. W., Mieyal, J. J., and Qin, J. (1998) Reactivity of the Human Thioltransferase (Glutaredoxin) C7S, C25S, C78S, C82S Mutant and NMR Solution Structure of Its Glutathionyl Mixed Disulfide Intermediate Reflect Catalytic Specificity. *Biochemistry 37*, 17145–17156.
17. Discola, K. F., de Oliveira, M. A., Cussiol, J. R. R., Monteiro, G., Bárcena, J. A., Porras, P., Padilla, C. A., Guimarães, B. G., and Netto, L. E. S. (2009) Structural Aspects of the Distinct Biochemical Properties of Glutaredoxin 1 and Glutaredoxin 2 from *Saccharomyces cerevisiae*. *J. Mol. Biol. 385*, 889–901.
18. Bushweller, J. H., Åslund, F., Wüthrich, K., and Holmgren, A. (1992) Structural and Functional Characterization of the Mutant *Escherichia coli* Glutaredoxin(C14S) and Its Mixed Disulfide with Glutathione. *Biochemistry 31*, 9288–9293.
19. Björnberg, O., Østergaard, H., and Winther, J. R. (2006) Mechanistic Insight Provided by Glutaredoxin within a Fusion to Redox-Sensitive Yellow Fluorescent Protein. *Biochemistry 45*, 2362–2371.
20. Holmgren, A. (1976) Hydrogen Donor System for *Escherichia coli* Ribonucleoside-Diphosphate Reductase Dependent upon Glutathione. *Proc. Natl. Acad. Sci. U.S.A. 73*, 2275–2279.
21. Peltoniemi, M. J., Karala, A.-R., Jurvansuu, J. K., Kinnula, V. L., and Ruddock, L. W. (2006) Insights into Deglutathionylation Reactions. Different Intermediates in the Glutaredoxin and Protein Disulfide Isomerase Catalyzed Reactions Are Defined by the γ-Linkage Present in Glutathione. *J. Biol. Chem. 281*, 33107–33114.
22. Nordstrand, K., Åslund, F., Meunier, S., Holmgren, A., Otting, G., and Berndt, K. D. (1999) Direct NMR Observation of the Cys-14 Thiol Proton of Reduced *Escherichia coli* Glutaredoxin-3 Supports the Presence of an Active Site Thiol-Thiolate Hydrogen Bond. *FEBS Lett. 449*, 196–200.
23. Tewari, Y. B., and Goldberg, R. N. (2003) Thermodynamics of the Oxidation-Reduction Reaction {2 Glutathione$_{red}$(aq) + NADP$_{ox}$(aq) = Glutathione$_{ox}$(aq) + NADP$_{red}$(aq)}. *J. Chem. Thermodyn. 35*, 1361–1381.
24. Jensen, K. S., Hansen, R. E., and Winther, J. R. (2009) Kinetic and Thermodynamic Aspects of Cellular Thiol-Disulfide Redox Regulation. *Antioxid. Redox Signaling 11*, 1047–1058.
25. Pace, C. N., Vajdos, F., Fee, L., Grimsley, G., and Gray, T. (1995) How to Measure and Predict the Molar Absorption Coefficient of a Protein. *Protein Sci. 4*, 2411–2423.
26. Wiseman, T., Williston, S., Brandts, J. F., and Lin, L.-N. (1989) Rapid Measurement of Binding Constants and Heats of Binding Using a New Titration Calorimeter. *Anal. Biochem. 179*, 131–137.
27. Bundle, D. R., and Sigurskjold, B. W. (1994) Determination of Accurate Thermodynamics of Binding by Titration Microcalorimetry. *Methods Enzymol. 247*, 288–305.
28. Riddles, P. W., Blakeley, R. L., and Zerner, B. (1983) Reassessment of Ellman's Reagent. *Methods Enzymol. 91*, 49–60.
29. Plotnikov, V. V., Brandts, J. M., Lin, L.-N., and Brandts, J. F. (1997) A New Ultrasensitive Scanning Calorimeter. *Anal. Biochem. 250*, 237–244.
30. Bruylants, G., Wouters, J., and Michaux, C. (2005) Differential Scanning Calorimetry in Life Sciences: Thermodynamics, Stability, Molecular Recognition and Application in Drug Design. *Curr. Med. Chem. 12*, 2011–2020.
31. Freire, E., Luque, I., and Townsend, B. (2001) ASACalc v1.2: Calculation of Accessible Surface Areas, Biocalorimetry Center, Johns Hopkins University.
32. Lee, B., and Richards, F. M. (1971) The Interpretation of Protein Structures: Estimation of Static Accessibility. *J. Mol. Biol. 55*, 379–400.
33. Fling, S. P., and Gregerson, D. S. (1986) Peptide and Protein Molecular Weight Determination by Electrophoresis Using a High-Molarity Tris Buffer System without Urea. *Anal. Biochem. 155*, 83–88.
34. Goldberg, R. N., Kishore, N., and Lennen, R. M. (2002) Thermodynamic Quantities for the Ionization Reactions of Buffers. *J. Phys. Chem. Ref. Data 31*, 231–370.
35. Murphy, K. P., and Freire, E. (1992) Thermodynamics of Structural Stability and Cooperative Folding Behavior in Proteins. *Adv. Protein Chem. 43*, 313–361.
36. Gan, Z.-R., Sardana, M. K., Jacobs, J. W., and Polokoff, M. A. (1990) Yeast Thioltransferase—The Active Site Cysteines Display Differential reactivity. *Arch. Biochem. Biophys. 282*, 110–115.
37. Mieyal, J. J., Starke, D. W., Gravina, S. A., and Hocevar, B. A. (1991) Thioltransferase in Human Red Blood Cells: Kinetics and Equilibrium. *Biochemistry 30*, 8883–8891.
38. Yang, Y., and Wells, W. W. (1991) Identification and Characterization of the Functional Amino Acids at the Active Center of Pig Liver Thioltransferase by Site-Directed Mutagenesis. *J. Biol. Chem. 266*, 12759–12765.
39. Rabenstein, D. L. (1973) Nuclear Magnetic Resonance Studies of the Acid-Base Chemistry of Amino Acids and Peptides. I. Microscopic Ionization Constants of Glutathione and Methylmercury-Complexed Glutathione. *J. Am. Chem. Soc. 95*, 2797–2803.
40. Nelson, J. W., and Creighton, T. E. (1994) Reactivity and Ionization of the Active Site Cysteine Residues of DsbA, a Protein Required for Disulfide Bond Formation in Vivo. *Biochemistry 33*, 5974–5983.
41. Baker, B. M., and Murphy, K. P. (1996) Evaluation of Linked Protonation Effects in Protein Binding Reactions Using Isothermal Titration Calorimetry. *Biophys. J. 71*, 2049–2055.
42. Elgán, T. H., and Berndt, K. D. (2008) Quantifying *Escherichia coli* Glutaredoxin-3 Substrate Specificity Using Ligand-induced Stability. *J. Biol. Chem. 283*, 32839–32847.
43. Rost, J., and Rapoport, S. (1964) Reduction-Potential of Glutathione. *Nature 201*, 185.
44. Åslund, F., Berndt, K. D., and Holmgren, A. (1997) Redox Potentials of Glutaredoxins and Other Thiol-Disulfide Oxidoreductases of the Thioredoxin Superfamily Determined by Direct Protein-Protein Redox Equilibria. *J. Biol. Chem. 272*, 30780–30786.
45. Sagemark, J., Elgán, T. H., Bürglin, T. R., Johansson, C., Holmgren, A., and Berndt, K. D. (2007) Redox Properties and Evolution of Human Glutaredoxins. *Proteins 68*, 879–892.
46. Østergaard, H., Tachibana, C., and Winther, J. R. (2004) Monitoring Disulfide Bond Formation in the Eukaryotic Cytosol. *J. Cell Biol. 166*, 337–345.
47. Gilbert, H. F. (1990) Molecular and Cellular Aspects of Thiol-Disulfide Exchange. *Adv. Enzymol. Relat. Areas Mol. Biol. 63*, 69–172.
48. Szajewski, R. P., and Whitesides, G. M. (1980) Rate Constants and Equilibrium Constants for Thiol-Disulfide Interchange Reactions Involving Oxidized Glutathione. *J. Am. Chem. Soc. 102*, 2011–2026.